Supplement of Atmos. Chem. Phys., 19, 2361–2384, 2019
https://doi.org/10.5194/acp-19-2361-2019-supplement

Atmospheric Chemistry and Physics
Open Access

Supplement of

High Arctic aircraft measurements characterising black carbon vertical variability in spring and summer

Hannes Schulz et al.

Correspondence to: Andreas B. Herber (andreas.herber@awi.de)

1 Supplementary results

1.1 Stratification of the polar dome

Figure S1 shows profiles of pressure and CO mixing ratio as function of potential temperature. Strong changes in potential temperature within narrow pressure intervals mark stable stratified zones and hence boundaries between different air masses in the polar dome. CO mixing ratios had a decreasing trend with altitude/potential temperature in spring while mixing ratios increased in summer. ΔCO is calculated as the difference of measured CO mixing ratios and the altitude dependent background value estimated as the fifth percentile of all measured CO mixing ratios within a potential temperature interval.

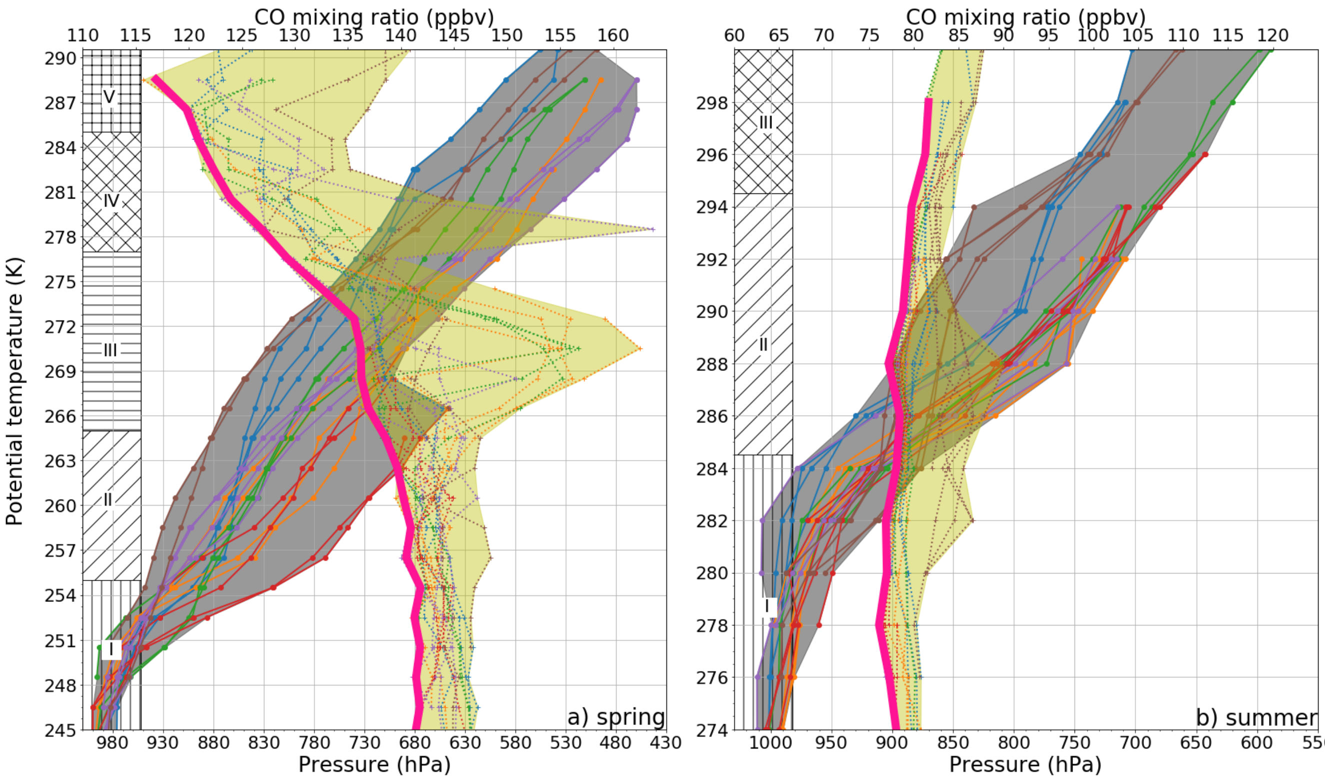

Supplemental Figure S1. Vertical profiles of pressure (lines in grey shading) and CO mixing ratio (lines in yellow shading) versus potential temperature for spring (a) and summer (b). Hatch patterns indicate the extent of the atmospheric levels defined in Sec. 3. The thick pink line marks the fifth percentile of measured CO mixing ratios which is assumed to represent the background concentrations in each potential temperature interval.

1.2 Transport to level IV of the spring polar dome

Level IV of the spring time polar dome over the High Canadian Arctic was affected by complex transport patterns. The patterns affecting the measurements from the two regions Alert (7 to 9 April) and Eureka (11 to 13 April) changed over time and were not continuously active. In order to discern different source regions, Fig. S2 shows trajectory overpass frequencies split up for the two periods. Contours in Fig. S2(b, d) indicate the frequency of liquid and ice cloud water encounters along the trajectories (see below).

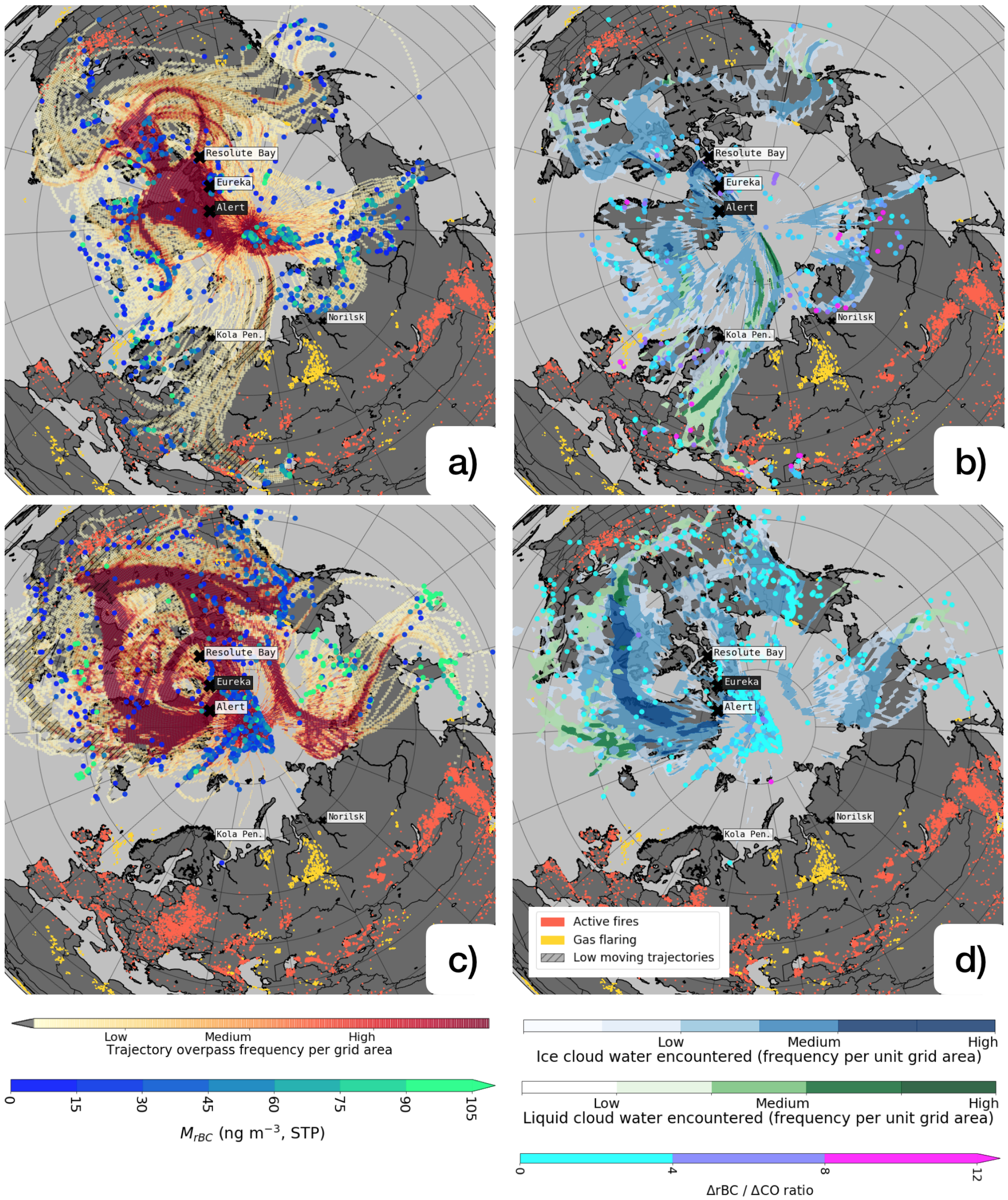

Supplemental Figure S2. Heat maps of normalised back–trajectory overpass frequencies (left) in each $0.5^\circ \cdot 0.5^\circ$ grid cell for flights of the spring campaign initialised within potential temperature level IV for profile flights from the two regions Alert (top) and Eureka (bottom). Green and blue contours (right) indicate the frequency of liquid and ice cloud water, respectively, encounters by the trajectories. Dots at the end point of trajectories, 10 days back in time, are colour coded with M_{rBC} (left) and R_{CO} (right) measured in flight. The aircraft operated near the stations marked with black labels. The map further shows MODIS active fire detections for the period 10 days prior to the first flight until the day of the last flight (orange dots) and known gas flaring sites (yellow dots) from the ECLIPSE emission inventory.

1.3 Cloud water encountered on trajectory paths

Based on the ECMWF operational data used in the kinematic back–trajectory model LAGRANTO, gridded frequencies of air parcels along the trajectories pathways with liquid and ice cloud water were calculated. Fig. S3 and S4 show those for spring and summer, respectively.

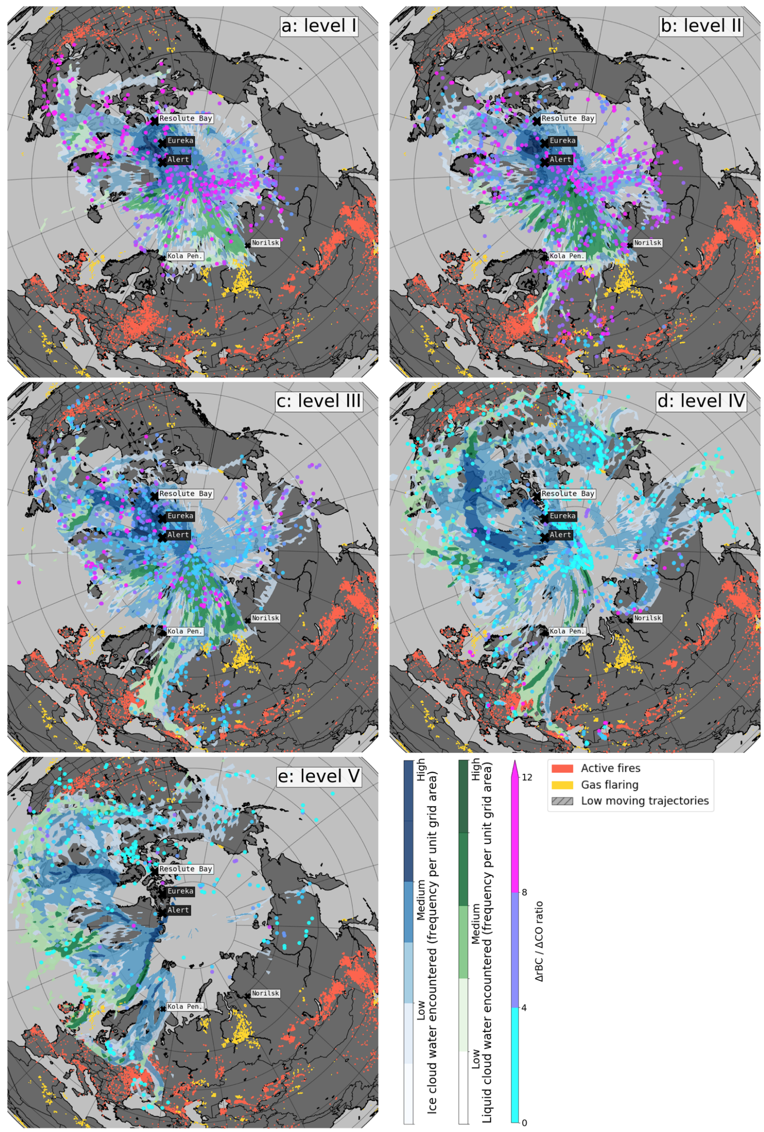

Supplemental Figure S3. Green and blue contours indicate encounters of liquid and ice cloud water, respectively, along the trajectories as frequencies in each $0.5^\circ \times 0.5^\circ$ grid cell. The trajectories were initialised at flight positions from the spring campaign in five potential temperature levels of the polar dome. Dots at the end point of trajectories, 10 days back in time, are colour coded with R_{CO} measured in flight. The aircraft operated near the stations marked with black labels. The map further shows MODIS active fire detections for the period 10 days prior to the first flight until the day of the last flight (orange dots) and known gas flaring sites (yellow dots) from the ECLIPSE emission inventory.

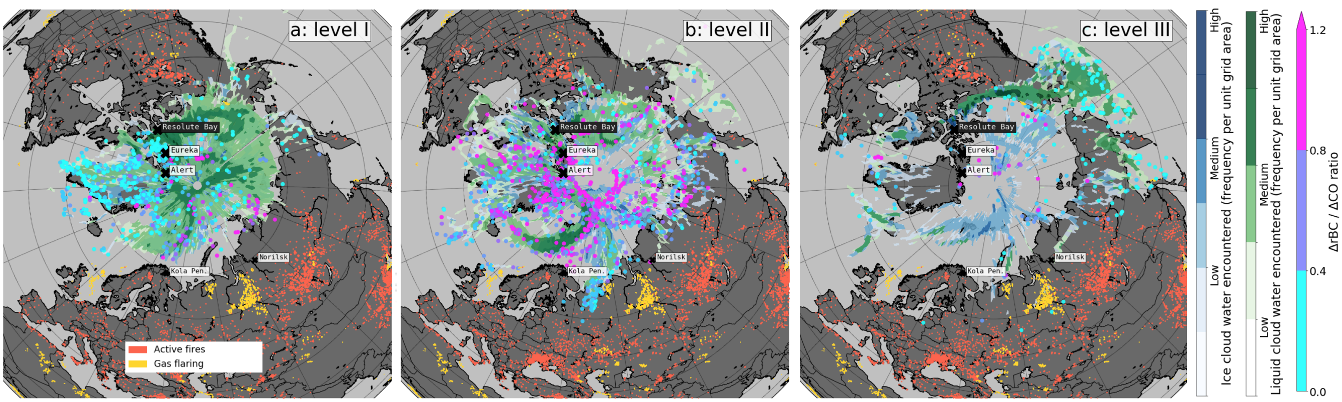

Supplemental Figure S4. Green and blue contours indicate encounters of liquid and ice cloud water, respectively, along the trajectories as frequencies in each $0.5^\circ \times 0.5^\circ$ grid cell. The trajectories were initialised at flight positions from the summer campaign in three potential temperature levels of the polar dome. Dots at the end point of the trajectories, 10 days back in time, are colour coded with R_{CO} measured in flight. The aircraft operated near the stations marked with black labels. The map further shows MODIS active fire detections for the period 10 days prior to the first flight until the day of the last flight (orange dots) and known gas flaring sites (yellow dots) from the ECLIPSE emission inventory.